Bull. Mater. Sci. (2019) 42:208
https://doi.org/10.1007/s12034-019-1904-3
© Indian Academy of Sciences

Effect of non-180° polarization invariants on the exchange bias of tetragonal ⟨001⟩ and rhombohedral ⟨111⟩ orientations of bismuth ferrite epitaxial thin films

M M SAJMOHAN[1], R RANJITH[1,*] and J A CHELVANE[2]
[1]Department of Materials Science and Metallurgical Engineering, IIT Hyderabad, Sangareddy, Kandi 502285, India
[2]Defence Metallurgical Research Laboratory, DRDO Hyderabad, Kanchanbagh 500066, India
*Author for correspondence (ranjith@iith.ac.in)

MS received 2 February 2019; accepted 30 March 2019

Abstract. $BiFeO_3$ (BFO) is the only room temperature multiferroic material that has been extensively studied due to its multifunctional properties. BFO with a canted G-type antiferromagnetic (AFM) ordering exhibits strong exchange bias characteristics with NiFe which offers the potential to design and utilize devices working based on multiferroic features. In the past, it was known that the presence of 180° domain walls of BFO hinders a plausible exchange bias interaction. To understand the role of the strain-induced effects on such 180° domain walls and its effect on the exchange bias, NiFe, a soft ferromagnetic layer, was grown on the epitaxial BFO AFM layers. An approximately 80 nm BFO layer was grown epitaxially in both the tetragonal (001) phase on the $LaAlO_3$ (001) substrate and the rhombohedral (111) phase on the $SrTiO_3$ (111) substrate, with a thin (10 nm) layer of $Ni_{80}Fe_{20}$ on top of it. An exchange bias of 510 Oe was observed in the tetragonal phase of BFO with a c/a ratio of 1.22, which is comparable with the exchange bias shown by the (111) oriented rhombohedral phase (360 Oe). Both the tetragonal (001) and rhombohedral (111) layers possess ferroelectric polarization normal to the sample surface and so the domain walls are mostly 180° oriented which is expected to have a minimum effect on the exchange bias. However, the weak strain-induced structural variants in the (111) oriented rhombohedral BFO and the monoclinic distortion present in the tetragonal BFO introduce non-180° domain walls in the system. These variants arising due to the structural distortion are expected to play a key role in defining the ferroelectric domain wall nature, thereby exhibiting exchange bias characteristics.

Keywords. Epitaxy; multiferroics; exchange bias; PLD.

1. Introduction

Multiferroic materials possessing magnetic and ferroelectric ordering simultaneously have been the main focus of research in the field of oxide electronics. The magnetoelectric coupling in the system facilitates an additional control on the operation of the devices [1,2]. Bismuth ferrite (BFO) is the only known single-phase material with room temperature multiferroic features (ferroelectric $T_C \sim 1100$ K and G-type antiferromagnetic (AFM) $T_N \sim 640$ K). BFO possesses an incommensurate spin cycloidal magnetic ordering with its propagation vector and periodicity of 62–64 nm along $\langle 01\bar{1} \rangle$, with all its Fe^{3+} electron spins aligning in a canted G-type AFM arrangement [3,4]. Moreover, single-layer BFO has been extensively studied with epitaxial thin films grown on a variety of substrates with a wide range of achievable strain, leading to various properties and structures [5,6]. These include the formation of rhombohedral structures to super-tetragonal structures owing to the strain induced by the substrates [7–9]. BFO is particularly important considering its use in a variety of applications in the field of data storage owing to its large polarization, magnetoelectric sensors and in other fields [5–11]. For compensated AFM surfaces of perovskite multiferroic materials, the exchange bias [12] is explained through various interactions like the Dzyaloshinskii–Moriya (D–M) interaction, the standard super-exchange at the interface [13], interactions facilitated through the roughness effect, pinning of AFM spins by the FE domain wall, etc. [14–17]. In rhombohedral systems, exchange bias scales with a density of 109 and 71° domain walls which pin the AFM domain wall and mostly depend on the domain wall density in the system. The room temperature AFM ordering of BFO with the week magnetoelectric coupling through the D–M interaction facilitates its utilization and electric field control of magnetism through exchange bias studies. In BFO, it has also been demonstrated that the FE domains are strongly coupled to the AFM domains and can be altered by switching the FE switching [18–20]. Also, in the case of rhombohedral BFO with the (111) oriented sample, it has the majority of 180° domain walls and minimum exchange bias due to the high compensation of spins on the surface [21]. However, the strain-induced structural variants in the samples can induce the non-180° domain walls

Published online: 28 June 2019

in the epitaxially grown thin films. It has been reported that the tetragonal BFO, known to possess the majority of 180° domain walls along with 90° domain walls without any structural distortions possesses negligible exchange bias [22]. In case of the tetragonal crystal structure, the polarization direction is ⟨001⟩, and so the domain walls are mostly 180° oriented along with possible 90° domain walls which contributes minimum to the exchange bias. The external electric field control on magnetism in the tetragonal crystal has been demonstrated on Fe/$BaTiO_3$, where the 180° magnetization reversal has been demonstrated [23]. Any deviation from the tetragonal nature will induce the non-180° domain walls with uncompensated spins, which induces an exchange bias between BFO and other soft ferromagnetic thin films. In this study, we explore the role of structural distortion in tetragonal (001) and rhombohedral (111) oriented epitaxial BFO in the exchange bias. The structural distortions in the BFO are expected to change the nature of the ferroelectric domains and affect the interface exchange interactions. The monoclinic distortion in tetragonal BFO will possess non-180° domain walls in addition to 180° domain walls to reduce the strain energy. Also, the structural variant in the (111) oriented rhombohedral BFO would also possess non-180° domain walls along with the 180° domain walls on the surface of epitaxial BFO. These variations induce the uncompensated spins in the interface and expected to induce exchange bias interaction. For measuring the role of strain and structural variations of BFO on exchange bias, we sputter-deposited a well-studied soft ferromagnetic and non-magnetostrictive NiFe thin film on top of the epitaxial BFO film to study the spontaneous exchange bias behaviour.

2. Experimental

Epilayers of BFO were grown on $SrTiO_3$ (STO) (001), (011), (111) and $LaAlO_3$ (LAO) (001) (MTI corporation inc.) single crystal substrates using the pulsed laser deposition (PLD) technique (coherent, KrF, $\lambda = 248$ nm, repetition rate of 3 Hz, fluence $\sim$2 J cm^{-2}) at a deposition rate of 0.07 Å per pulse. The depositions were carried out at 100 mTorr oxygen ambience and a growth temperature of $\sim$700°C. The samples are then cooled down to room temperature at a rate of 3° min^{-1}. The high-resolution X-ray diffraction (Bruker, D8 discover) (θ–2θ, reciprocal space mapping (RSM)) was carried out to confirm epitaxy and strain in the epilayers. The piezoresponse force microscopy (PFM) studies were carried out in the piezoresponse mode (dimension icon: Bruker). Platinum–iridium-doped n-type silicon conductive tips are used for the ferroelectric domain imaging, by applying a 500 mV alternating current bias applied between the conductive tip and the bottom electrode. To study the exchange bias, an $\sim$10 nm NiFe was sputter-deposited at room temperature on top of the BFO thin films with a deposition rate of 0.03 Å s^{-1}. The room temperature magnetic hysteresis was measured using a vibrating sample magnetometer (M/s Lakeshore, Cryotronics, USA) with the field applied parallel to the sample surface to find the spontaneous exchange bias.

3. Results and discussion

Figure 1 shows the X-ray diffraction (XRD) pattern of the phase pure BFO epilayers with respective substrate orientations on the STO and LAO substrates [24]. The out-of-plane lattice parameter was $\sim$4.05 Å for the (100) oriented film grown on STO and 4.64 Å on top of the LAO substrate, which are higher compared to pseudo-cubic BFO layers (3.960 Å). No impurities were detected (within limits of XRD) in any of the thin films deposited using PLD. The orientation relations of the epilayers were confirmed with the ϕ scans (shown as an inset in figure 1), performed on both film and substrates. The cube-on-cube growth and the symmetry of the film were thus confirmed. In case of the (111) oriented BFO, two different domain variants were observed. This would cause the polarization vector to possess an in-plane component along with the out-of-plane components. This splitting of the (111) domain is clearly visible in asymmetric RSM analysis and is unique for the rhombohedral system.

RSM was performed on asymmetric (21$\bar{1}$) planes of BFO grown on the STO (111) substrate. It is known that the splitting of the (111) and (222) peaks confirms the rhombohedral symmetry with monoclinic M_A type distortion [25]. The BFO/STO (111) film was completely strained as the pseudomorphic line passes through the film and substrate reflection.

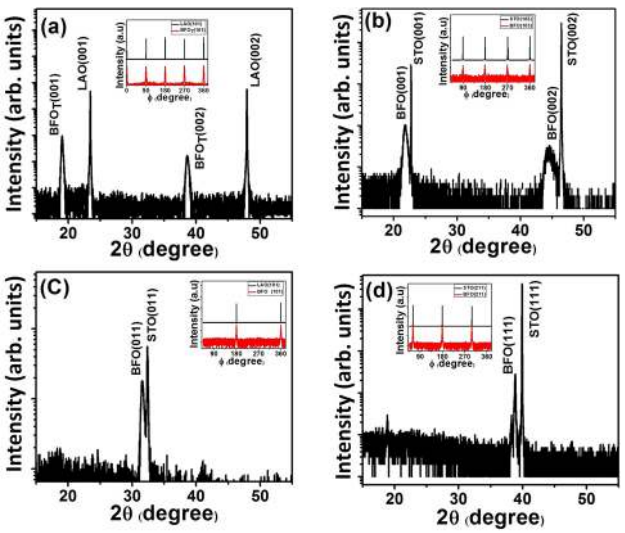

Figure 1. (**a**) XRD and ϕ scan along the (101) plane of the BFO tetragonal phase grown on the LAO substrate. (**b**) XRD and ϕ scan of the STO (103) plane along with the BFO (103) plane of the BFO/STO grown in the (001) direction. (**c**) XRD and ϕ scan along the (002) plane of the BFO/STO (011) sample. (**d**) XRD and ϕ scan along the (211) plane of the BFO/STO (111) sample. All the samples are phase pure and symmetry is preserved.

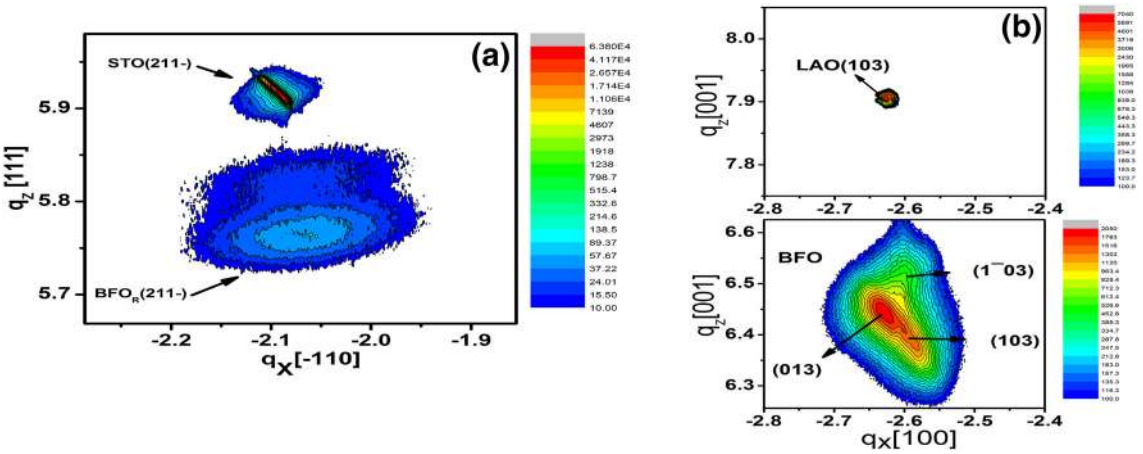

Figure 2. Small area asymmetric RSM scan performed on (**a**) the $(21\bar{1})$ asymmetric plane of BFO/STO (111) shows the rhombohedral splitting and (**b**) the $(10\bar{3})$ asymmetric plane of BFO/LAO (001) shows the weak monoclinic distortion.

The clear splitting of the BFO (111) domain indicates a distorted rhombohedral structure which is also observed in the normal XRD profile. This splitting of the structural domains will induce the formation of non-180° domain walls in the BFO ⟨111⟩ thin films. Figure 2b shows the combined mesh scans around the $(10\bar{3})$ reflection of the LAO substrate and that of the epitaxially grown tetragonal BFO film. The film is grown fully strained with an in-plane lattice parameter of 3.79 Å. This confirms the tetragonal nature of the highly strained BFO films with a large c/a ratio of 1.22. In case of the monoclinic distortion, the $h0\,l$ plane will split into three domains and hhl will split into two domains (hkl), being the miller indices representing the plane [26]. The clear splitting of the (103) domains in figure 2b shows the monoclinic distortion present in the tetragonal BFO. The presence of such low symmetry monoclinic distortions has been observed in earlier reports [27].

Figure 3 represents the room temperature M–H curve for the different orientations of the film with an ∼10 nm polycrystalline $Ni_{80}Fe_{20}$ sputter-deposited on top of the BFO thin films. The exchange bias effect is found to be different in the three differently oriented samples and is high in the (110) oriented sample as reported by Bai *et al* [25]. The origin of magnetic anisotropy arises in the BFO, as the spin cycloidal propagation vector is in the ⟨$01\bar{1}$⟩ direction, and is having the maximum exchange bias as reported earlier. A spontaneous exchange bias of −1290, −960 and −360 Oe was observed in the case of the (110), (001) and (111) oriented samples, respectively.

The exchange bias studies on the tetragonal BFO grown on the LAO (001) substrate was found to be of −510 Oe, which is comparable to the BFO_R with the (111) orientation (−360 Oe was observed). The tetragonal BFO with a large c/a ratio of 1.22 is known to possess magnetic spins oriented in a combination of C-type and G-type AFM structures [28]. Because BFO is magnetoelectric, the magnetic and ferroelectric domains are expected to be of the same magnitude [29].

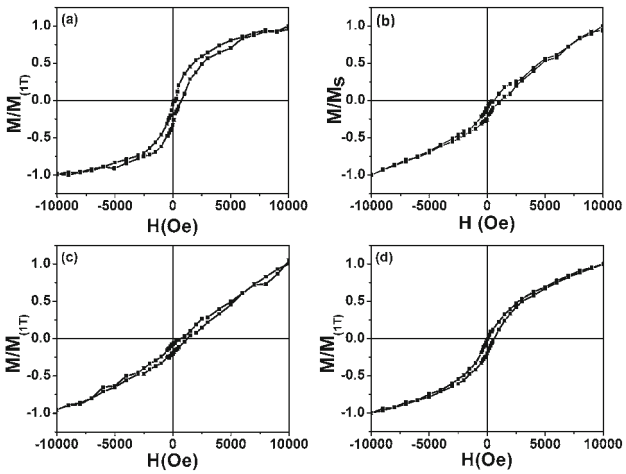

Figure 3. Normalized magnetic hysteresis loops for samples measured at room temperature with an applied field parallel to the sample surface: (**a**) NiFe/(BFO_T/LAO (001)), (**b**) NiFe/(BFO/STO (001)), (**c**) NiFe/(BFO/STO (011)) and (**d**) NiFe/(BFO/STO (111)).

The PFM studies on tetragonal BFO films were associated with 180 and 90° domain walls with dominating out-of-plane polarization components. The 90° domain walls of tetragonal BFO form to minimize the elastic energy in the strained film along with the monoclinic distortion [30]. The observed ferroelectric domain patterns of the rhombohedral (111) orientation and tetragonal BFO in the (001) orientation are shown in figure 4.

The BFO_R (111)/STO and BFO_T (001)/LAO possess a dominant out-of-plane polarization component and a large number of 180° domains. However, the presence of 180° domain walls is known to have a high compensation of spin moments in BFO in comparison with the 71 and 109° domain walls [26]. In spite of the presence of 180° domains, structural variants arising due to the strain in both BFO_R (111) and BFO_T (001) give rise to the formation of domain walls

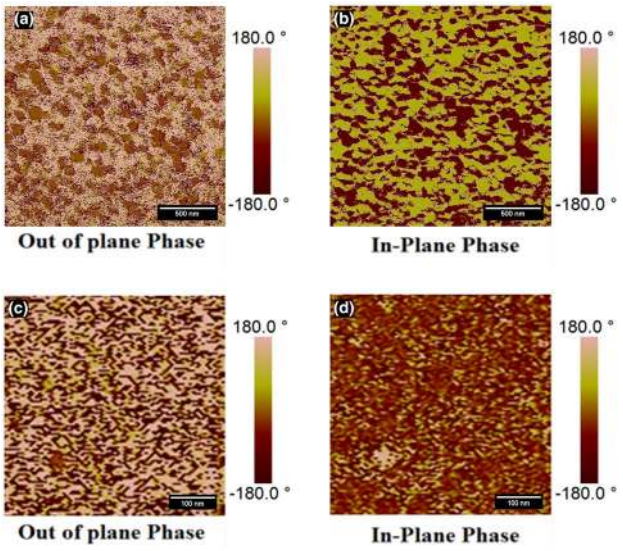

Figure 4. (**a** and **b**) In-plane and out-of-plane phase images of BFO/LSMO/STO (111), respectively; (**c** and **d**) represent the in-plane and out-of-plane phase images of BFOT/LSMO/LAO (001), respectively.

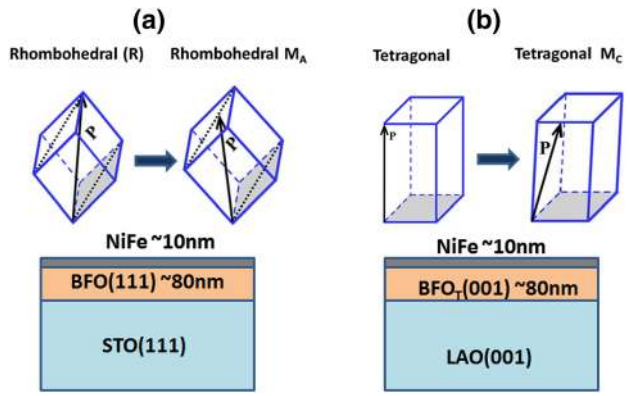

Figure 5. Schematic representation of (**a**) the monoclinic M_A type distortion of rhombohedral BFO and (**b**) the monoclinic M_C type distortion in tetragonal BFO. The change in the polarization direction is represented by the vector **P**.

apart from 180° domain walls. There is a possibility of having 24 different domain variants in case of the monoclinic M_A and/or M_C type crystal structure, and accordingly, the types of domain walls. Figure 5 shows the schematics of the sample configuration with thickness and the corresponding monoclinic type distortions present in the sample.

The observed structural distortions and the planar strain were also evident from the RSM studies in both the samples. The presence of such structural distortions is also reflected in the formation of domains with varying facets. From the out-of-plane phase image of the tetragonal sample, it is evident that the 90° domains are formed along with the striped 180° domains. The average domain periodicity calculated in the reign of striped domain formations is in the range of 50 nm with the minimum domain size varying from 25 to 30 nm in the tetragonal sample. The average domain size of the rhombohedral BFO (111) is around 45 nm. Also, the exchange bias decreases with the AFM domain size which is coupled to the ferroelectric domains in the case of the multiferroic BFO. The formation of non-180° domains is evident and 90° domains are also formed along with the closure domains. The presence of such mixed domains originating from the structural distortions present in both tetragonal and rhombohedral phases of BFO contributes to the uncompensated spin moments leading to exchange bias. It is evident from the PFM domain studies that the domain wall and crystal structure tunability are plausible and could facilitate the fabrication of BFO-based multifunctional devices.

4. Conclusion

BFO epilayers (∼80 nm) were grown on STO with various orientations and LAO (001) substrates. Fully strained growth of the BFO was observed on STO and LAO substrate. The tetragonal phase having a weak monoclinic distortion with a c/a ratio of 1.22 was grown on top of the LAO substrate in the (001) direction. The weak monoclinic distortion in the tetragonal phase and the domain variant present in the rhombohedral (111) sample are evident from RSM analysis. A spontaneous exchange bias of 510 and 360 Oe was evident in the tetragonal-like BFO sample and rhombohedral BFO oriented in the ⟨111⟩ direction, respectively. The magnitude of the exchange bias observed for the (111) oriented BFO films and the tetragonal BFO (001) films was not negligible, and it is due to the co-existence of non-180° domain walls present in the sample surface because of the structural distortion induced by the substrate strain. The presence of structural distortions in both the tetragonal and rhombohedral phases of BFO is expected to induce uncompensated spins in the BFO layers and facilitate exchange bias interaction.

Acknowledgements

This work was supported by DAE-BRNS (project no: 34/20/05/2014-BRNS).

References

[1] Reohr W, Honigschmid H, Robertazzi R, Gogl D, Pesavento F, Lammers S *et al* 2002 *IEEE Circuits Devices Mag.* **18** 17
[2] Binek C and Doudin B 2005 *J. Phys. Condens. Matter* **17** 39
[3] Wang J, Neaton J B, Zheng H, Nagarajan V, Ogale S B, Liu B *et al* 2003 *Science* **299** 1719
[4] Bertinshaw J, Maran R, Callori S J, Ramesh V, Cheung J, Danilkin S A *et al* 2016 *Nat. Commun.* **7** 12664
[5] Zhang J X, Xiang B, He Q, Seidel J, Zeches R J, Yu P *et al* 2009 *Science* **326** 977
[6] Ramesh R and Spaldin N A 2007 *Nature Mater.* **6** 2

[7] Sajmohan M M, Bandyopadhyay S, Jogi T, Bhattacharya S and Ramadurai R 2019 *J. Appl. Phys.* **125** 012501
[8] Sajmohan M M, Sreenath M V and Ranjith R *MRS Adv.* **3** 2713
[9] Sajmohan M M and Ranjith R 2018 *AIP Conf. Proc.* **1942** 80040
[10] Choi T, Lee S, Choi Y J, Kiryukhin V and Cheong S W 2009 *Science* **324** 63
[11] Chu S H, Singh D J, Wang J, Li E P and Ong K P 2012 *Laser Photonics Rev.* **6** 684
[12] Nogules J and Schuller I K 1999 *J. Magn. Magn. Mater.* **192** 203
[13] Dong S, Yamauchi K, Yunoki S, Yu R, Liang S, Moreo A *et al* 2009 *Phys. Rev. Lett.* **103** 5
[14] Bea H, Bibes M, Cherifi S, Nolting F, Warot-Fonrose B, Fusil S *et al* 2006 *Appl. Phys. Lett.* **89** 242114
[15] Martin L W, Chu Y H, Zhan Q, Ramesh R, Han S J, Wang S X *et al* 2007 *Appl. Phys. Lett.* **91** 1
[16] Bea H, Bibes M, Ott F, Dupe B, Zhu X H, Petit S *et al* 2008 *Phys. Rev. Lett.* **100** 1
[17] Dho J and Blamire M G 2009 *J. Appl. Phys.* **106** 1
[18] Heron J T, Schlom D G and Ramesh R 2014 *Appl. Phys. Rev.* **1** 21303
[19] Dho J and Blamire M G 2009 *J. Appl. Phys.* **106** 73914
[20] Zhao T, Scholl A, Zavaliche F, Lee K, Barry M, Doran A *et al* 2006 *Nat. Mater.* **5** 823
[21] Bai F, Yu G, Wang Y, Jin L, Zeng H, Tang X *et al* 2012 *Appl. Phys. Lett.* **101** 092401
[22] Xu Q, Yuan X, Xue X, Shi Z, Wen Z and Du J 2014 *Phys. Status Solidi B* **251** 892
[23] Venkataiah G, Anupama S, Katsuyoshi K, Mitsuru I and Tomoyasu T 2017 *Phys. Status Solidi RRL* **11** 1700294
[24] Bea H, Bibes M, Barthlmy A, Bouzehouane K, Jacquet E, Khodan A *et al* 2005 *Appl. Phys. Lett.* **87** 1
[25] Li J, Wang J, Wuttig M, Ramesh R, Wang N, Ruette B *et al* 2004 *Appl. Phys. Lett.* **84** 5261
[26] Saito K, Ulyanenkov A, Grossmann V, Ress H, Bruegemann L, Ohta H *et al* 2006 *Jpn. J. Appl. Phys.* **45** 7311
[27] Zhang N, Yokota H, Glazer A M, Ren Z, Keen D A, Keeble D S *et al* 2014 *Nat. Commun.* **5** 5231
[28] Hatt A J, Spaldin N A and Ederer C 2010 *Phys. Rev. B* **81** 54109
[29] Martin L W, Chu Y H, Holcomb M B, Huijben M, Yu P, Han S J *et al* 2008 *Nano Lett.* **8** 2050
[30] Dipanjan M, Vilas S, Milko I, Stephen J, Amit K, Kalinin S V *et al* 2010 *Nano Lett.* **10** 2555